

Application Report

Electrophysiological characterization of human iPSC-derived motor neurons using Qube 384 and QPatch

Studies of culture duration, biophysical properties and neurological disease phenotyping

Summary

Human induced pluripotent stem cells (hiPSCs) were developed a decade ago and hold great promise for disease modelling, drug discovery and personalized medicine, especially in cardiac and neurological diseases¹. Dysfunctional ion channels are one of the major targets in these diseases and thus, as the iPSC technology improves, a requirement arises for instrumentation that can characterize electrophysiological properties of iPSCs in a high-throughput fashion. Here, we demonstrate the use of the automated patch clamp (APC) platforms Qube 384 and QPatch in three characterization studies of hiPSC motor neurons derived from patients and healthy individuals. The results include:

- APC recording of hiPSC-derived motor neurons with high success rates on Qube (60%) and QPatch (30%)
- Biophysical characterization of voltage-gated channels, Na⁺ (Na_v) and K⁺ (K_v), in healthy hiPSCs
- Measurements of a ligand-gated channel (GABA_A receptor) in healthy control cells
- Screening of hiPSC motor neurons derived from Spinal Muscular Atrophy (SMA) and Amyotrophic Lateral Sclerosis (ALS) patients
- Comparison of hiPSC motor neurons derived from two different healthy individuals

Introduction

hiPSCs were discovered in 2007 when it was shown for the first time that the somatic cells of a patient could be reprogrammed into an embryonic pluripotent state^{2,3}. Once the cells have been reprogrammed to hiPSCs they can be differentiated into cell types, like cardiomyocytes and neurons⁴, which show great

potential in disease modelling, drug discovery and personalized medicine^{5,6}. However, quality control during hiPSC reprogramming and differentiation as well as standardization of hiPSC-derived cell lines, are areas that are still under development⁸. Thus, there is a strong requirement for high-throughput methodologies for characterization and screening of hiPSC-derived cell lines.

Ion channels represent attractive therapeutic targets in the nervous and cardiovascular systems⁷ rendering electrophysiological studies of hiPSC-derived cell lines interesting for their usage in drug discovery. Here we present three electrophysiological characterization studies of hiPSC-derived motor neurons using the APC platforms, Qube 384 and QPatch, with up to 60% success rates:

1. In the first sample study, we characterize the ion channel content of hiPSC motor neurons derived from a healthy individual. The study includes the pharmacological dissection of endogenous ion channels (Na_v and K_v), identification of a ligand-gated receptor (GABA_A) and a measure of current amplitude and experiment success rate versus time in culture.
2. In the second sample study, we utilized the high-throughput nature of our system for parallel screening of two disease models, using hiPSC neurons derived from SMA or ALS patients, together with control cells from healthy subjects and isogenic control cells.
3. In the third sample study, we evaluate the variability of Na_v channel biophysical properties between hiPSC motor neurons derived from two different healthy individuals.

Results

Screening hiPSC-derived motor neurons using automated patch clamp

The major challenge when investigating neurons using APC platforms is the requirement to dissociate the cells from their neuronal network while maintaining cell viability and membrane integrity⁹. By optimization of the harvest- and whole-cell protocols we have overcome this obstacle resulting in success rates of up to 60% using our 384 well APC system Qube (fig. 1).

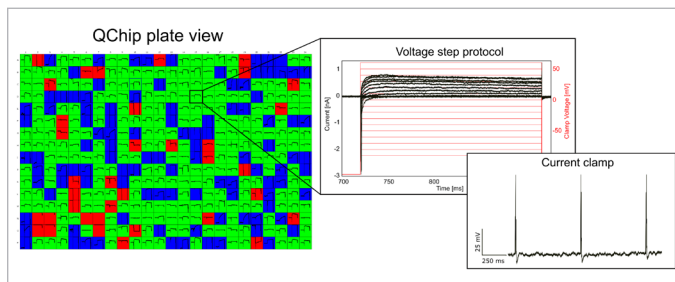


Fig. 1: High throughput measurements of hiPSC-derived motor neurons on Qube. Overview of the 384 well QChip illustrating the high-throughput nature of Qube measurements yielding up to 60% success rates (cell resistance > 200 M Ω). The color coding corresponds to passed (green) or failed (red and blue) experiments. The system allows us to perform voltage- and paced current-clamp protocols within the same experiment.

On our medium-throughput system QPatch, we obtained up to 30% success rates. Quantification of Na_V - and K_V - channel current-voltage (IV) relationships yielded very similar results on the two systems (fig. 2).

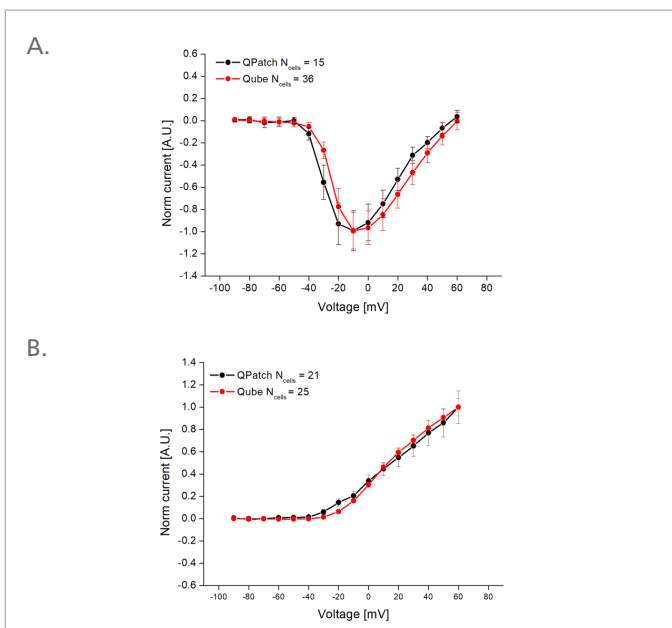


Fig. 2: QPatch and Qube measurements on hiPSC-derived motor neurons yielded similar current-voltage (IV) relationship of Na_V and K_V channels. The IV relationships of Na_V and K_V channels were quantified by stepping from -90 mV to +60 mV ($\Delta V = +10$ mV) on QPatch (black) and Qube (red). A: Average Na_V current (normalized to the current recorded at -10 mV) versus step voltage. B: Average K_V current (normalized to the current recorded at +60 mV). All error bars are SEM.

Sample study 1: Electrophysiological characterization of hiPSC-derived motor neurons

Characterization of hiPSC-derived motor neurons included Na_V- and K_V- channel IV-relationship (fig. 2), addition of channel blockers (fig. 3) and recordings of currents induced by the addition of γ -aminobutyric acid (GABA) (fig. 4).

For all experiments, neurons with a whole-cell resistance (R_{mem}) below 200 M Ω were excluded from the data analysis. Of these cells ($N = 645$ cells) $98\% \pm 2\%$ expressed K_V channels and $85\% \pm 3\%$ expressed Na_V channels (K_V and Na_V current amplitudes above 150 pA). The K_V currents clustered in two subpopulations, one carrying characteristics of the A-type K_V channel and the other exhibiting properties known for delayed rectifier K_V channels (fig. 3A).

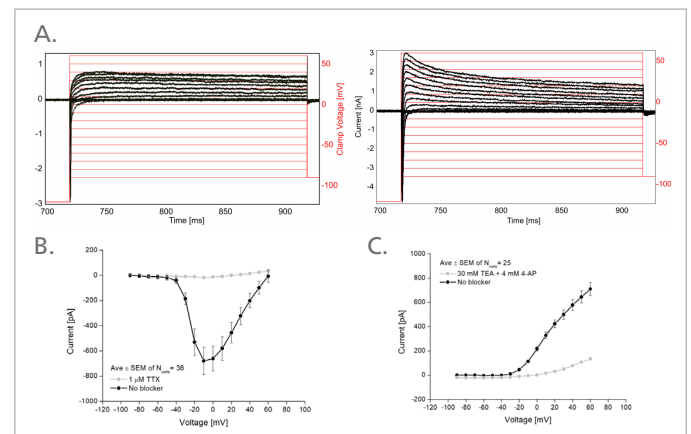


Fig. 3: IV relationship of Na_V and K_V channels in hiPSC-derived motor neurons. A: Representative current responses (black) to a voltage step protocol (red) when stepping from -90 mV to +60 mV ($\Delta V = +10$ mV), showing that the cells expressed Na_V channels and a mixture of delayed rectifier and A-type K_V channels. B: Average current-voltage relationship of Na_V peak currents. The current was fully blocked by subsequent addition of 1 μ M TTX. C: Average K_V current-voltage relationship. Addition of 30 mM TEA and 4 mM 4-AP resulted in a $\sim 85\%$ block at +60 mV. Error bars are SEM.

Using our standard ligand application with washout after 30 s (fig. 4A) and stacked ligand application with rapid washout after 0.8 s (fig. 4B) we added 100 μ M GABA to the neurons at a holding potential of -90 mV. GABA-induced currents were detected in $\sim 45\%$ of the cells.

Upon thawing a vial of BrainXell cryopreserved hiPSC neural progenitors, they require a week maturation in culture. During this time the cells are differentiated into functional post-mitotic motor neurons, creating a neuronal dendritic network (fig. 5A). Quantifying Na_V-, K_V- and GABA channel currents as a function of culturing days *in vitro* (DIV) (fig. 5B) revealed that the current amplitudes of these channels increase over time. However, the simultaneous development of the dendritic network challenges the harvesting procedure thereby lowering overall success rate (fig. 5C). Thus, when optimizing an hiPSC assay for a specific ion channel target, the best compromise between channel expression and experiment success rate should be found in order to ensure the best results.

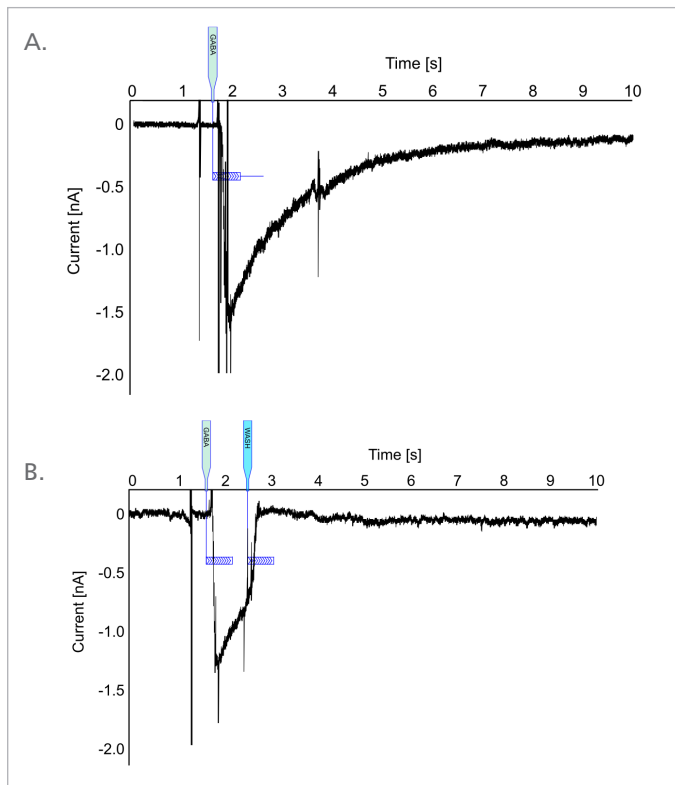


Fig. 4: Recordings of currents induced by γ -aminobutyric acid (GABA). Current response recorded at a holding potential of -90 mV upon the addition of $100 \mu\text{M}$ GABA. A: Standard ligand application with washout after 30 s. B: Stacked ligand application, in which ligand and wash solutions are stacked in the same pipette, ensuring rapid washout after 0.8 s. This approach can help to mitigate current desensitization in an experiment with repeated ligand stimulation.

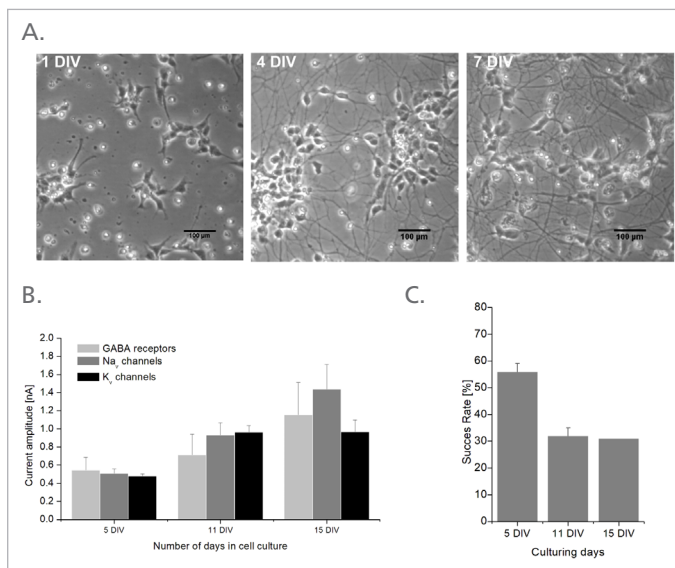


Fig. 5: Current amplitudes increase and the success rate decreases as a function of culturing days *in vitro* (DIV). A: Light micrographs of hiPSC progenitor neurons differentiating into functional post-mitotic motor neurons, captured at 1 DIV, 4 DIV and 7 DIV. Scale bars are $100 \mu\text{m}$. B: Current amplitudes recorded at 5 DIV, 11 DIV and 15 DIV for GABA receptor channels (light grey, $V = -90$ mV), Na_v channels (grey, $V = 0$ mV) and K_v channels (black, $V = 40$ mV). C: Percentage success rate ($R_{\text{mem}} > 200 \text{ M}\Omega$) at 5 DIV, 11 DIV and 15 DIV. Error bars are SEM.

Sample study 2: Screening of hiPSC motor neurons derived from SMA and ALS patients

To demonstrate the feasibility of Qube 384 for characterization and drug screening of central nervous system disorders we used hiPSCs from SMA¹⁰ or ALS¹¹ patients and compared their electrophysiological properties to the control cell lines (fig. 6 - 8).

For the SMA hiPSCs, the biophysical parameters of Na_v and K_v channels were compared to control hiPSCs from a healthy individual. In addition, a batch of SMA hiPSCs was treated on 1 DIV and 4 DIV with $1 \mu\text{M}$ of the compound SMN-C3^{12,13}, which is currently in phase I clinical trials for treatment of SMA. A sample layout for the parallel measurement of control, SMA and SMA+SMN-C3 neurons is displayed in figure 6. To test several cell clones in parallel we used a cell-clone cell transfer plate (ccCTP) having four cell suspension compartments. The final layout of the experiment plate (QChip) was the following (fig. 6):

- Control neurons (row 1-8)
- SMA neurons (row 9-12)
- SMA neurons cultured with $1 \mu\text{M}$ SMN-C3 (row 13-16)

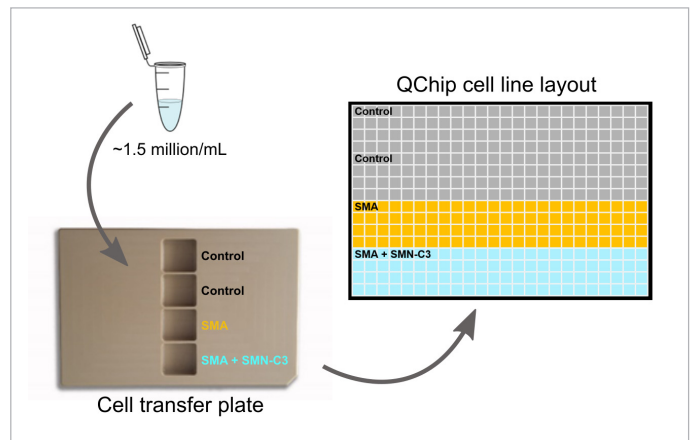


Fig. 6: Experiment layout for test of compound effects on SMA iPSCs. $680 \mu\text{L}$ cell suspension with a cell density of 1.5 million/mL was added to each of the four compartments of the cell transfer plate (CTP). The resulting experiment layout on the QChip: control neurons (row 1-8), SMA neurons (row 9-12) and SMA neurons cultured with $1 \mu\text{M}$ SMN-C3 (row 13-16).

The K_v IV relationship revealed similar activity in all tested cell lines (data not shown). However, the Na_v IV relationship of the SMA neurons displayed, as previously shown¹⁰, a significantly increased maximum Na_v current as compared to the control (fig. 7A and B, orange). Culturing the SMA cells in the presence of $1 \mu\text{M}$ of the compound SMN-C3 completely rescued the increased Na_v peak current (fig. 7A and B, blue). No significant differences were recorded between the voltage at half-maximal activation ($V_{1/2}$) between the cell lines (fig. 7C and D). Furthermore, no change in cell capacitance was detected (data not shown).

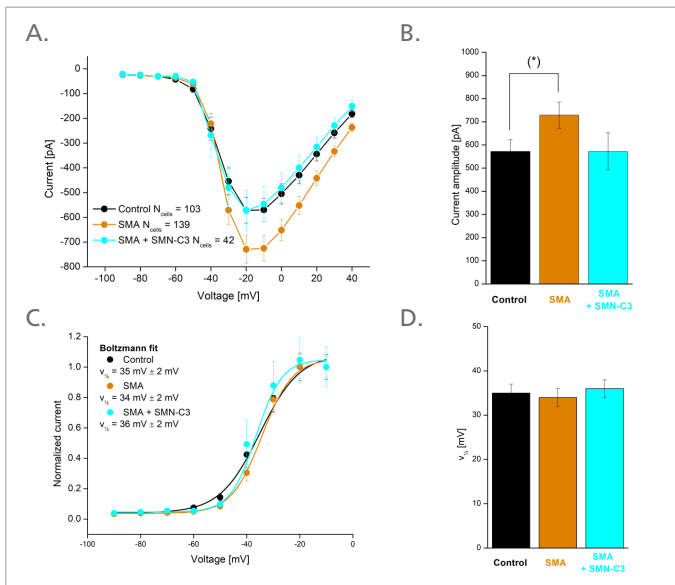


Fig. 7: Evaluation of compound effects on Na_v channel properties in SMA neurons. Parallel recordings of control neurons (black), SMA neurons (orange) and SMA neurons treated with SMN-C3 during culturing (blue). A: Average Na_v current versus step voltage. B: Quantification of the current amplitude at -20 mV. The current amplitude is significantly larger in SMA cells than in control cells (students t-test, $p < 0.05$ (*), 95% confidence interval) C: Average Na_v current normalized to the current recorded at $V = -20$ mV. Fitting of a Boltzmann function (solid lines) yielded the half-activation voltage ($V_{1/2}$). D: Half-activation voltage ($V_{1/2}$) values. Error bars are SEM.

The ALS neurons were shown to contain a single disease-causing point mutation in the SOD1 gene (ALS D90A)¹¹. Here we tested in parallel control neurons, ALS neurons (ALS D90A) as well as an isogenic control (ALS D90D) (fig. 8). We recorded a significantly increased Na_v peak current in ALS D90A neurons as compared to the control neurons, which could be rescued by a single point mutation in the SOD1 gene of the isogenic cell line, ALS D90D (fig. 8A and B). No significant differences were recorded between the voltage at half-maximal activation ($V_{1/2}$) between the cell lines (fig. 8C and D).

Note that the hiPSC technology is still lacking a standardized hiPSC state and that quality control during reprogramming and differentiation protocols, which might introduce genetic variability, remains an area under development⁸. Therefore, we recommend comparing control and disease cells from several individuals, for which the genetic integrity of the hiPSCs has been validated, before drawing any strong conclusions.

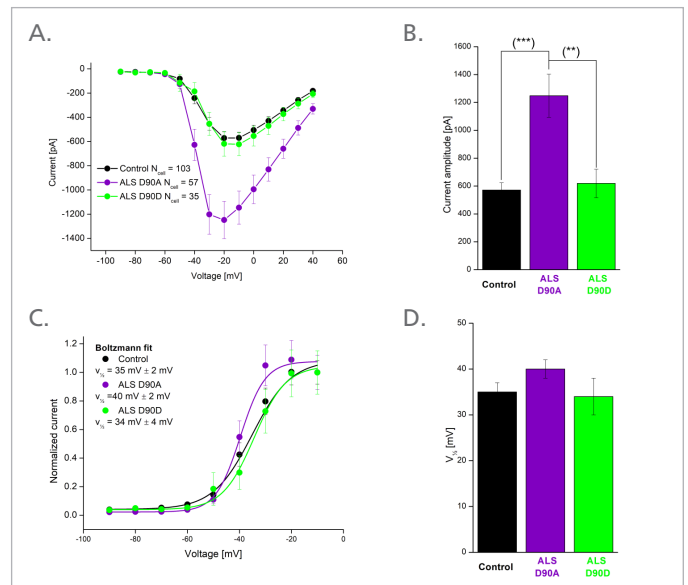


Fig. 8: Evaluation of Na_v channel properties in ALS neurons. Parallel recordings of control (black), ALS D90A (purple) and isogenic rescue, ALS D90D (green) neurons. A: Average Na_v current versus step voltage. B: Quantification of the current amplitude at -20 mV. The current amplitude is significantly larger in ALS D90A cells than in control cells (students t-test, $p < 0.001$ (***) 95% confidence interval) or ALS D90D cells (students t-test, $p < 0.01$ (**), 95% confidence interval). C: Average Na_v current normalized to the current recorded at $V = -20$ mV. Fitting of a Boltzmann function (solid lines) yielded the half-activation voltage ($V_{1/2}$). D: Half-activation voltage ($V_{1/2}$) values. Error bars are SEM.

Sample study 3: Characterization of Na_v channel variability between hiPSC motor neurons derived from two different healthy individuals.

As an initial indicator of the reproducibility of electrophysiological phenotypes between different hiPSC clones, we performed a parallel characterization of Na_v channel properties in hiPSC motor neurons derived from two different healthy individuals, cell source 1 and 2, respectively.

To avoid contributions from K_v channels, the experiments were performed without K^+ in the intra- and extra-cellular solutions and to eliminate Ca_v currents, 0.2 mM CdCl_2 was added to the extracellular solution. Na_v currents were evoked using the same voltage protocol as for the previously presented Na_v IV plots (fig. 9A) and revealed significant differences in both current amplitude and half-activation voltage ($V_{1/2}$) between the two cell sources (see fig. 9B and C).

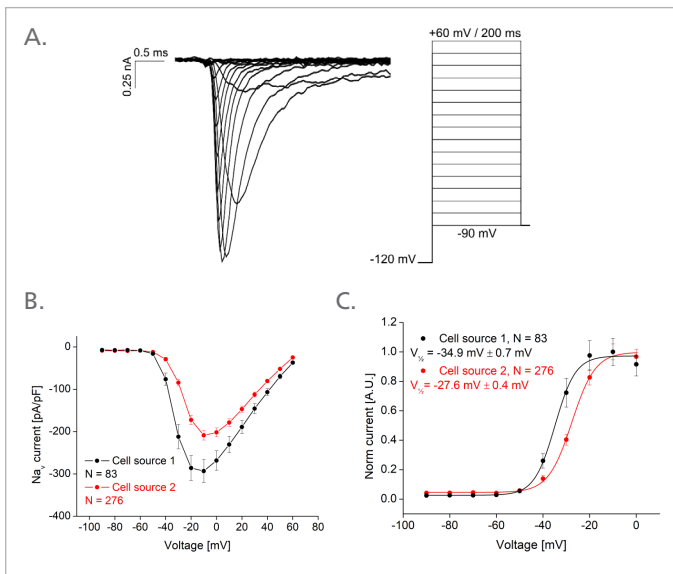


Fig. 9: Activation of Na_v current in hiPSC-derived motor neurons from two different healthy individuals. A: Representative Na_v current response (left) evoked by step depolarizations in +10 mV increments from -90 mV to +60 mV (right). B: The average Na_v current versus voltage was normalized to cell capacitance and plotted for cell source 1 (black) and cell source 2 (red). C: Na_v current were normalized to the current recorded at -15 mV for cell source 1 (black) and cell source 2 (red). Fitting of a Boltzmann function (solid lines) yielded the half-activation voltage ($V_{1/2}$) of -34.9 mV \pm 0.7 mV and -27.6 mV \pm 0.4 mV for cell source 1 and cell source 2, respectively. Data points are average \pm SEM of recordings from 83 (cell source 1) or 276 (cell source 2) cells.

Na_v channel inactivation currents were evoked by step depolarization to +10 mV from different conditioning potentials (from -90 mV to 0 mV in +10 mV increments) (fig. 10A). Plotting the normalized inactivation current versus conditioning voltages (fig. 10B) revealed a significant right shift of the inactivation recorded in cell source 2 as compared to cell source 1. Na_v current recovery was quantified using 10 sequential depolarizations to +10 mV with a series of inter-pulse increments (Δt) starting at 1 ms and increasing with 50% each run of the voltage protocol (fig. 10C). The 2nd peak current amplitude was normalized to the 1st peak current amplitude and plotted as a function of Δt (fig. 10D). Fitting of a monoexponential function to the data revealed a significant difference between Na_v channel recovery in the two cell sources.

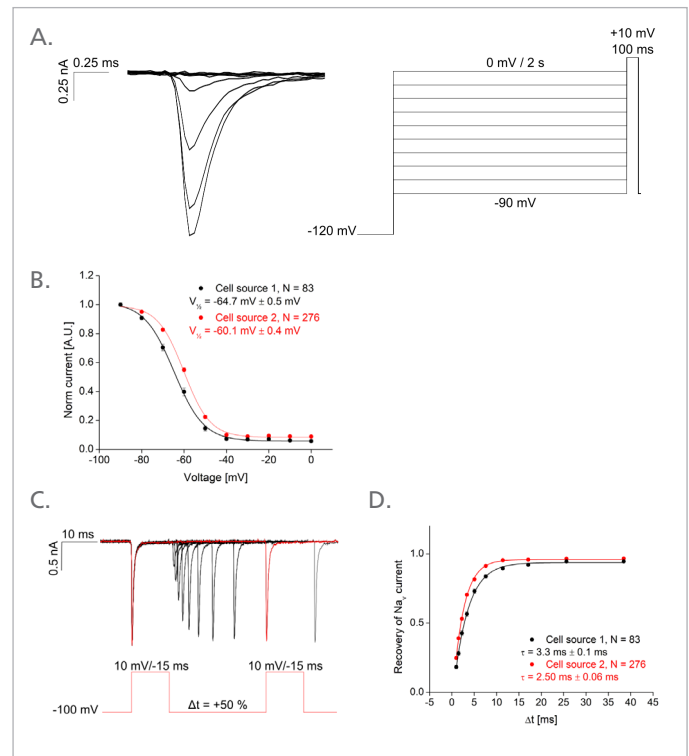


Fig. 10: Inactivation and recovery of Na_v currents in hiPSC-derived motor neurons from two different healthy individuals. A: Representative current response (left) evoked by step depolarization to +10 mV from different conditioning potentials (from -90 mV to 0 mV in 10 mV increments) (right). B: The Na_v current at the step depolarization (+10 mV) was normalized to the current evoked from the conditioning potential of -90 mV and plotted as a function of conditioning voltages. Fitting of a Boltzmann function (solid lines) yielded half-inactivation voltages ($V_{1/2}$) of -64.7 mV \pm 0.5 mV and -60.1 mV \pm 0.4 mV for cell source 1 (black) and cell source 2 (red), respectively. C: Representative Na_v current traces (top) upon 10 sequential depolarizations with a series of inter-pulse increments (Δt) starting at 1 ms and increasing with 50% each run of the voltage protocol (bottom). D: The recovery of the Na_v current was quantified by normalizing the 2nd peak current amplitude to the 1st peak current amplitude and plotting the normalized current as a function of Δt . Fitting of a monoexponential function to the data (solid lines) yielded time constants (τ) of 3.3 ms \pm 0.1 ms and 2.50 ms \pm 0.06 ms for cell source 1 (black) and cell source 2 (red), respectively. Data points are average \pm SEM between recordings from 83 (black) or 276 (red) cells.

The data show that there are small but significant variations in Na_v channel electrophysiology between hiPSC derived motor neurons from different healthy individuals. These might be caused by 1) differences in the genetic background, 2) clone variations in hiPSC differentiation efficiency or 3) line-to-line variations in hiPSC maturation. This variability has to be considered when studying hiPSC-derived disease models, in order to identify true pathophysiological phenotypes.

Conclusion

Our results demonstrate the feasibility of conducting electrophysiological characterization studies of hiPSC – derived motor neurons using APC systems, Qube 384 and QPatch, thus paving the way for high-throughput ion channel-targeted drug-screening, diagnostics and precision medicine for neurological disorders.

Methods

Cells: Spinal motor neurons were generated from the following human hiPSC lines: normal control (WC30), asymptomatic SMA carrier (GM03815), SMA Type I (GM00232), ALS with D90A SOD1 mutation, and D90D SOD1 isogenic control (ND29149). The D90D hiPSC line was established by correcting the D90A SOD1 mutation using TALEN technology¹¹. Directed differentiation was performed as described¹⁴. For the compound experiments 100 μ M SMN-C3 was pre-mixed with the culture medium to give a final concentration of 1 μ M and added at day 1 and day 4 *in vitro*. After 5-15 days culturing according to BrainXell protocols, the culture medium was removed, and the cells were washed x2 in PBS and harvested using 2 mL Accumax™ per T25 cell flask (incubate 7 min at 37°C). Subsequently 6 mL culture medium was added, and the cells were spun down (4 min, 150 x g) and resuspended in extracellular solution to achieve the required cell density.

Solutions: For intra- and extra-cellular solutions contact Sophion Bioscience A/S.

K_v and Na_v channel IV relationship: *Voltage protocol:* The protocol consisted of a 700 ms pre-step at -120 mV followed by 200 ms voltage steps from -90 mV to +60 mV ($\Delta V = +10$ mV). *Compounds:* Prior to the second run of the voltage protocol either 1 μ M TTX (Na_v block) or a combination of 30 mM TEA and 4 mM 4-AP (K_v block) were added to the cells. *Analysis:* Cells with membrane resistance $R_{mem} < 200$ M Ω and current amplitudes $I < 150$ pA were excluded from the analysis. The minimum Na_v peak current was extracted within a 2.5 ms time interval. The Na_v activation curves were created by normalizing the peak current to the amplitude at $V = -15$ mV. The average K_v current was extracted within a 30 ms time interval (starting at 890 ms).

GABA-induced currents: Ligand addition: 100 μ M GABA was added at a voltage $V = -90$ mV.

Na_v channel biophysical characterization: *Voltage protocols:* *Activation:* As described above. *Inactivation:* The protocol consisted of a 700 ms pre-step at -120 mV followed by 2 s voltage steps from -90 mV to 0 mV ($\Delta V = +10$ mV), each succeeded by a 100 ms step depolarization to +10 mV. *Recovery:* The protocol consisted of 10 sequential 10 ms depolarizations from -100 mV to -15 mV with a series of inter-pulse increments (Δt) starting at 1 ms and increasing with 50% each run. *Analysis:* Cells with membrane resistance $R_{mem} < 1000$ M Ω and current amplitudes $I < 200$ pA were excluded from the analysis. *Activation:* Analysis as described above. *Inactivation:* The minimum Na_v peak current at the last step depolarization of the protocol was extracted within a 2.5 ms time interval. The Na_v inactivation curves were created

by normalizing the peak current to the amplitude recorded at condition potential -90 mV. *Recovery:* The minimum Na_v peak current of the 2nd depolarization of the voltage protocol was extracted within a 2.5 ms time interval and normalized to the corresponding current amplitude of the 1st depolarization.

Acknowledgements

All cell lines were kindly provided by BrainXell Inc. and the authors would like to thank Mike Hendrickson (project manager, BrainXell Inc.) and Paul Guyett (postdoctoral scientist, BrainXell Inc.) for ongoing scientific support.

References:

1. Shi, Y., Inoue, H., Wu, J. C. & Yamanaka, S. Induced pluripotent stem cell technology: a decade of progress. *Nature Reviews Drug Discovery* 16, 115–130 (2017).
2. Yu, J. et al. Induced Pluripotent Stem Cell Lines Derived from Human Somatic Cells. *Science* 318, 1917–1920 (2007).
3. Takahashi, K. et al. Induction of Pluripotent Stem Cells from Adult Human Fibroblasts by Defined Factors. *Cell* 131, 861–872 (2007).
4. Bellin, M., Marchetto, M. C., Gage, F. H. & Mummery, C. L. Induced pluripotent stem cells: the new patient? *Nature Reviews Molecular Cell Biology* 13, 713–726 (2012).
5. Ko, H. C. & Gelb, B. D. Concise Review: Drug Discovery in the Age of the Induced Pluripotent Stem Cell. *STEM CELLS Translational Medicine* 3, 500–509 (2014).
6. Grskovic, M., Javaherian, A., Strulovici, B. & Daley, G. Q. Induced pluripotent stem cells — opportunities for disease modelling and drug discovery. *Nature Reviews Drug Discovery* 10, 915–929 (2011).
7. Dunlop, J., Bowlby, M., Peri, R., Vasilyev, D. & Arias, R. High-throughput electrophysiology: an emerging paradigm for ion-channel screening and physiology. *Nature Reviews Drug Discovery* 7, 358–368 (2008).
8. Popp, B. et al. Need for high-resolution Genetic Analysis in iPSC: Results and Lessons from the ForIPSC Consortium. *Scientific Reports* 8, (2018).
9. Raman, I. M. & Bean, B. P. Resurgent Sodium Current and Action Potential Formation in Dissociated Cerebellar Purkinje Neurons. *The Journal of Neuroscience* 17, 4517–4526 (1997).
10. Liu, H. et al. Spinal muscular atrophy patient-derived motor neurons exhibit hyperexcitability. *Scientific Reports* 5, (2015).
11. Chen, H. et al. Modeling ALS with iPSCs Reveals that Mutant SOD1 Misregulates Neurofilament Balance in Motor Neurons. *Cell Stem Cell* 14, 796–809 (2014).
12. Naryshkin, N. A. et al. SMN2 splicing modifiers improve motor function and longevity in mice with spinal muscular atrophy. *Science* 345, 688–693 (2014).
13. Cully, M. Beefing up the right splice variant to treat spinal muscular atrophy: Neuromuscular disorders. *Nature Reviews Drug Discovery* 13, 725–725 (2014).
14. Du, Z.-W. et al. Generation and expansion of highly pure motor neuron progenitors from human pluripotent stem cells. *Nature Communications* 6, (2015).

Author:

Kadla R Rosholm, Application scientist